

Phase diagram of spin-1 bosons on one-dimensional lattices

Matteo Rizzi,¹ Davide Rossini,¹ Gabriele De Chiara,¹ Simone Montangero,¹ and Rosario Fazio¹

¹ *NEST- INFN & Scuola Normale Superiore, Piazza dei Cavalieri 7, I-56126 Pisa, Italy**

(Dated: March 23, 2022)

Spinor Bose condensates loaded in optical lattices have a rich phase diagram characterized by different magnetic order. Here we apply the Density Matrix Renormalization Group to accurately determine the phase diagram for spin-1 bosons loaded on a one-dimensional lattice. The Mott lobes present an even or odd asymmetry associated to the boson filling. We show that for odd fillings the insulating phase is *always* in a dimerized state. The results obtained in this work are also relevant for the determination of the ground state phase diagram of the $S = 1$ Heisenberg model with biquadratic interaction.

PACS numbers: 03.75.Mn, 75.10.Pq, 73.43.Nq

The experimental realization of optical lattices [1] has paved the way to study strongly correlated many-particle systems with cold atomic gases (see e.g. [2, 3]). The main advantages with respect to condensed matter systems lie on the possibility of a precise knowledge of the underlying microscopic models and an accurate and relatively easy control of the various couplings. Probably one of the most spectacular experiments in this respect is the observation [4] of a Superfluid - Mott Insulator transition previously predicted in [5] by a mapping onto the Bose-Hubbard model [6].

More recently the use of far-off-resonance optical traps has opened the possibility to study spinor condensates [7]. Spin effects are enhanced by the presence of strong interactions and small occupation number, thus resulting in a rich variety of phases with different magnetic ordering. For spin-1 bosons it was predicted that the Mott insulating phases have nematic singlet [8] or dimerized [9] ground state depending on the mean occupation and on the value of the spin exchange. Since the paper by Demler and Zhou [8] several works have addressed the properties of the phase diagram of spinor condensates trapped in optical lattices [10, 11, 12, 13, 14, 15]. The increasing attention in spinor optical lattices has also revived the attention on open problems in the theory of quantum magnetism. The spinor Bose-Hubbard model, when the filling corresponds to one boson per site, can be mapped onto the $S = 1$ Heisenberg model with biquadratic interactions which exhibits a rich phase diagram including a long debated nematic to dimer quantum phase transition [16, 17, 18, 19, 20, 21, 22, 23].

Up to now the location of the phase boundary of the spinor Bose-Hubbard model has been determined by means of mean-field and strong coupling approaches. A quantitative calculation of the phase diagram is however still missing. This might be particularly important in one dimension where non-perturbative effects are more pronounced. This is the aim of this Letter. We determine the location of the Mott lobes showing the even/odd asymmetry in the spinor case discussed in [8]. We then discuss the magnetic properties of the first lobe, concluding

that it is always in a dimerized phase.

The effective Bose-Hubbard Hamiltonian, appropriate for $S = 1$ bosons, is given by

$$\hat{\mathcal{H}} = \frac{U_0}{2} \sum_i \hat{n}_i(\hat{n}_i - 1) + \frac{U_2}{2} \sum_i (\hat{\mathbf{S}}_i^2 - 2\hat{n}_i) - \mu \sum_i \hat{n}_i - t \sum_{i,\sigma} \left(\hat{a}_{i,\sigma}^\dagger \hat{a}_{i+1,\sigma} + \hat{a}_{i+1,\sigma}^\dagger \hat{a}_{i,\sigma} \right). \quad (1)$$

The operator $\hat{a}_{i,\sigma}^\dagger$ creates a boson in the lowest Bloch band localized on site i and with spin component σ along the quantization axis: $\hat{n}_i = \sum_\sigma \hat{a}_{i,\sigma}^\dagger \hat{a}_{i,\sigma}$ and $\hat{\mathbf{S}}_i = \sum_{\sigma,\sigma'} \hat{a}_{i,\sigma}^\dagger \mathbf{T}_{\sigma,\sigma'} \hat{a}_{i,\sigma'}$ are the total number of particles and the total spin on site i (\mathbf{T} are the spin-1 operators). Atoms residing on the same lattice site have identical orbital wave function and their spin function must be symmetric. This constraint imposes that $S_i + n_i$ must be even. The uniqueness of the completely symmetric state with fixed spin and number makes it possible to denote the single site states with $|n_i, S_i, S_i^z\rangle$. The coupling constants, which obey the constraint $-1 < U_2/U_0 < 1/2$, can be expressed in terms of the appropriate Wannier functions [10]. U_0 is set as the energy scale unit: $U_0 = 1$. We discuss only the anti-ferromagnetic case ($0 < U_2 < 1/2$).

In the absence of spin dependent coupling a qualitative picture of the phase diagram can be drawn starting from the case of zero hopping ($t = 0$). The ground state is separated from any excited state by a finite energy gap. For finite hopping strength, the energy cost to add or remove a particle ΔE_\pm (excitation gap) is reduced and at a critical value $t_c^\pm(\mu)$ vanishes. This phase is named the Mott insulator. For large hopping amplitudes the ground state is a globally coherent superfluid phase. When U_2 is different from zero, states with lowest spins, compatible with the constraint $n_i + S_i = \text{even}$, are favoured. This introduces an even/odd asymmetry of the lobes: the amplitude of lobes with odd filling is reduced as compared with the lobes corresponding to even fillings [8]. In the first lobe the extra energy required to have two particles on a site (instead of one) is $1 + 2U_2 - \mu$, thus lowering the chemical potential value where the second lobe

starts. On the other hand, having no particles on a site gives no gain due to spin terms, accounting for the nearly unvaried bottom boundary of the lobe.

In order to determine the phase diagram of Eq.(1) we use the finite-size Density Matrix Renormalization Group (DMRG) with open boundary conditions [24]. The strategy of the DMRG is to construct a portion of the system (called the system block) and then recursively enlarge it, until the desired system size is reached. At every step the basis of the corresponding Hamiltonian is truncated, so that the size of the Hilbert space is kept manageable as the physical system grows. The truncation of the Hilbert space is performed by retaining the eigenstates corresponding to the m highest eigenvalues of the block's reduced density matrix.

The DMRG has been employed, for the spinless case, in [25, 26]. The presence of the spin degree of freedom makes the analysis considerably more difficult. In the numerical calculations the Hilbert space for the on-site part of the Hamiltonian is fixed by imposing a maximum occupation number \bar{n}_{max} . As the first lobe is characterized by an insulating phase with $n = 1$ particle per site we choose $\bar{n}_{max} = 3$ in this case; the dimension of the Hilbert space per site becomes $d = 20$. We have checked, by increasing the value of \bar{n}_{max} , that this truncation of the Hilbert space is sufficient to compute the first lobe. In each DMRG iteration we keep up to $m = 300$ states in order to guarantee accurate results. The numerical calculations of the second lobe ($n = 2$ particles per site) have been performed with $\bar{n}_{max} = 4$ (which corresponds to $d = 35$).

Phase Diagram - In the insulating phase the first excited state is separated by the ground state by a Mott gap. In the limit of zero hopping the gap is determined by the extra energy ΔE_{\pm} needed to place/remove a boson at a given site. The finite hopping renormalizes the gap which will vanish at a critical value. Then the system becomes superfluid. This method has been employed for the spinless case by Freericks and Monien [27], and in [25, 26] where it was combined with the DMRG. Here we use it for the spinor case. Three iterations of the DMRG procedure are performed, with projections on different number sectors; the corresponding ground states give the desired energies E_0 , $E_{\pm} = E_0 + \Delta E_{\pm}$. As target energies we used those obtained by the mapping of the Bose-Hubbard system into effective models as described in [10]. We considered chains up to $L = 128$ sites for the first lobe, and $L = 48$ for the second lobe. The extrapolation procedure to extract the asymptotic values was obtained by means of linear fit in $1/L$, as discussed in [26]. A comparison with a quadratic fit shows that $O(1/L^2)$ corrections are negligible on the scale of Fig.1.

The plot of the phase diagram in the (μ, t) plane for different values of the spin coupling U_2 is shown in Fig.1. The first lobe tends to reduce its size on increasing the spin coupling; in particular the upper critical chemical

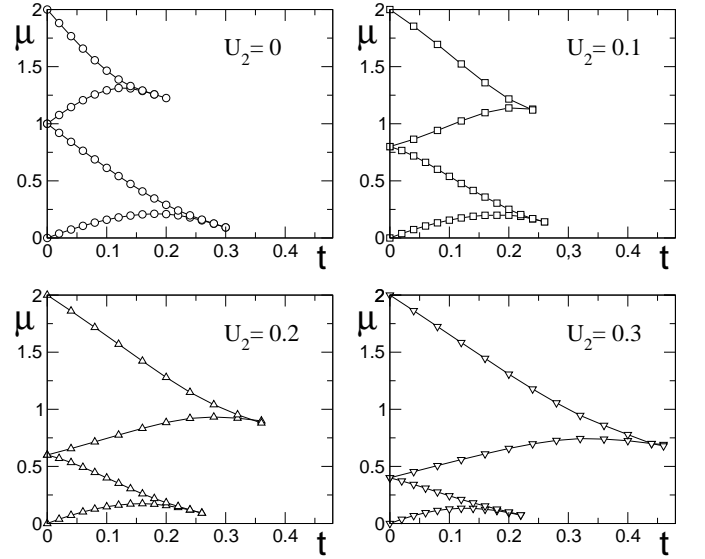


FIG. 1: Phase diagram for the first two lobes of the 1D Bose-Hubbard spin 1 model with nearest-neighbor interactions. The different panels correspond to different values of U_2 . The curves for $U_2 = 0$ coincide with the first two lobes for the spinless model computed in Refs.[25, 26].

potential at $t = 0$ is $\mu_c^+(0) = 1 - 2U_2$, while the t^* value of the hopping strength over which the system is always superfluid is suppressed as U_2 increases. On the other hand, the second lobe grows up when U_2 increases. This even/odd effect, predicted in [8], is quantified in Fig.1.

Magnetic properties of the first Mott lobe - The first lobe of the spinor Bose lattice has a very interesting magnetic structure. In presence of small hopping t boson tunneling processes induce effective pairwise magnetic interactions between the spins, described by Hamiltonian [10]:

$$\hat{\mathcal{H}}_{\text{eff}} = \kappa \sum_{\langle ij \rangle} \left[\cos \theta (\hat{\mathbf{S}}_i \cdot \hat{\mathbf{S}}_j) + \sin \theta (\hat{\mathbf{S}}_i \cdot \hat{\mathbf{S}}_j)^2 \right] \quad (2)$$

with

$$\tan \theta = \frac{1}{1 - 2U_2} \quad \kappa = \frac{2t^2}{1 + U_2} \sqrt{1 + \tan^2 \theta} \quad (3)$$

The absence of higher order terms, such as $(\hat{\mathbf{S}}_i \cdot \hat{\mathbf{S}}_j)^3$, is due to the fact that the product of any three spin operators can be expressed via lower order terms. In the case of anti-ferromagnetic interaction in Eq.(1), the parameter θ varies in the interval $\theta \in [-3/4\pi, -\pi/2[$. Because of the form of the magnetic Hamiltonian, each bond tends to form a singlet-spin configuration, but singlet states on neighboring bonds are not allowed. There are two possible ground states that may appear in this situation. A nematic state can be constructed by mixing states with total spin $S = 0$ and $S = 2$ on each bond. This construction

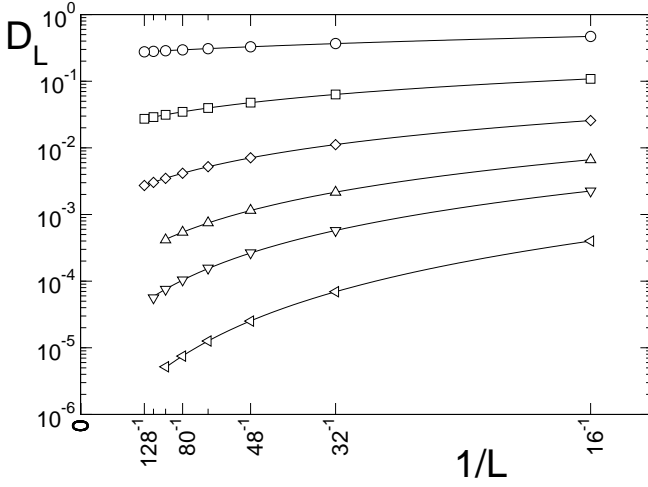


FIG. 2: Finite-size scaling of D_L for selected values of θ : circles ($\theta = -0.65\pi$), squares (-0.7π), diamonds (-0.72π), triangles up (-0.73π), triangles down (-0.735π), triangles left (-0.74π). In order to extrapolate the order parameter D , numerical data have been fitted with $D_L = D + cL^{-\alpha}$ (straight lines). DMRG simulations are performed with $m \simeq 140$ for $\theta > -0.73\pi$, and $m \simeq 250$ for $\theta \leq -0.73\pi$.

can be repeated on neighboring bonds, thereby preserving translational invariance. This state breaks the spin-space rotational group $O(3)$, though time-reversal symmetry is preserved. The expectation value of any spin operator vanishes ($\langle \hat{S}_i^\alpha \rangle = 0$, $\alpha = x, y, z$), while some of the quadrupole operators have finite expectation values. The tensor $Q^{ab} = \langle \hat{S}_i^a \hat{S}_i^b \rangle - \frac{2}{3} \delta^{ab}$ is a traceless diagonal matrix, due to invariance under spin reflections. Since it has two identical eigenvalues ($\langle (\hat{S}_i^x)^2 \rangle = \langle (\hat{S}_i^y)^2 \rangle \neq \langle (\hat{S}_i^z)^2 \rangle$), it can be written as $Q^{ab} = Q (d^a d^b - \frac{1}{3} \delta^{ab})$ using an order parameter $\langle \hat{Q} \rangle \equiv \langle (\hat{S}_i^z)^2 \rangle - \langle (\hat{S}_i^x)^2 \rangle = \frac{2}{3} (\langle (\hat{S}_i^z)^2 \rangle - 1)$ and a unit vector $\mathbf{d} = \pm \mathbf{z}$. However, since $[\hat{Q}, \hat{H}_{\text{eff}}] = 0$, it is not possible to get $Q \neq 0$ in finite-size systems, analogously to what happens for the magnetization without external field. Therefore we characterized the range of nematic correlations in the ground state by coupling this operator to a fictitious “nematic field”: $\hat{H}_\lambda = \hat{H}_{\text{eff}} + \lambda \hat{Q}$, and by evaluating the nematic susceptibility χ_{nem} as a function of L :

$$\chi_{\text{nem}} \equiv - \frac{d^2 E_0(\lambda)}{d\lambda^2} \Big|_{\lambda=0} = \sum_{\gamma} \frac{|Q_{0,\gamma}|^2}{E_\gamma - E_0}, \quad (4)$$

where $E_0(\lambda)$ is the ground energy of \hat{H}_λ , $Q_{0,\gamma}$ is the matrix element between the ground and an excited state of \hat{H}_{eff} (respectively with energy E_0 and E_γ).

On the other hand a possibility to have $SO(3)$ symmetric solution stems from breaking translational invariance. Indeed a dimerized solution with singlets on every second bond satisfy these requirements. Dimerization could be described looking at the differences in expecta-

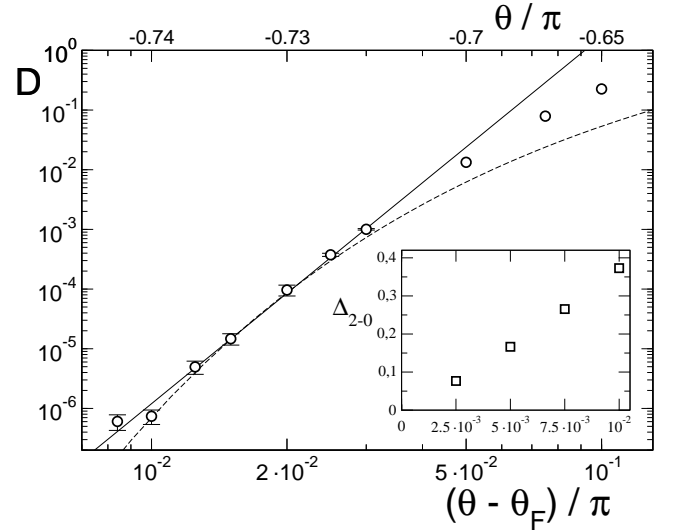


FIG. 3: Dimerization order parameter D near the ferromagnetic boundary: solid line shows a power law fit $D \sim (\theta - \theta_F)^\gamma$ of numerical data with $\gamma \simeq 6.15$; dashed line shows an exponential law fit $D \sim \exp[-a/(\theta - \theta_F)^{-1/2}]$ with $a \simeq 2.91$. The linear fit is done over data for $\theta < -0.7\pi$, while the exponential fit is for $\theta \leq -0.73\pi$. DMRG calculations are performed with up to $m \simeq 300$ states. Inset: extrapolated scaled gap $\Delta_{2-0} = (L-1)(E_2 - E_0)$ at the thermodynamic limit, close to θ_F .

tion values of pair Hamiltonian $\hat{\mathcal{H}}_{\text{eff}}^{(ij)}$ on adjacent links ($\hat{\mathcal{H}}_{\text{eff}} = \sum_{\langle ij \rangle} \hat{\mathcal{H}}_{\text{eff}}^{(ij)}$) [28]. The order parameter D reads

$$D \equiv \left| \langle \hat{\mathcal{H}}_{\text{eff}}^{(i-1,i)} \rangle - \langle \hat{\mathcal{H}}_{\text{eff}}^{(i,i+1)} \rangle \right|. \quad (5)$$

It has been proposed [16] that a narrow nematic region exists between the ferromagnetic phase boundary ($\theta_F = -3\pi/4$, i.e. $U_2 = 0$) and a critical angle $\theta_C \approx -0.7\pi$ (i.e. $U_2 \sim 10^{-2}$), whereas a dimerized solution is favoured in the remaining anti-ferromagnetic region $\theta_C \leq \theta \leq -\pi/2$. This implies that the dimerization order parameter D should scale to zero in the whole nematic region. This possibility has been analyzed in Ref. [18] where it was suggested that D might go to 0 exponentially near the ferromagnetic boundary, making it difficult to detect the effective existence of the nematic phase. This interesting challenge has motivated numerical investigations with different methods [18, 19, 21, 22]. We present new DMRG results which clarify the magnetic properties of the first Mott lobe (for sufficiently small hopping) and, consequently, of the biquadratic Heisenberg chain.

According to our numerical calculation there is *no* intermediate nematic phase, indeed we found a power law decay of the dimerization order parameter near $\theta_F = -3\pi/4$. The simulations of the bilinear-biquadratic model (2) are less time and memory consuming than Bose-Hubbard ones, since the local Hilbert space has a

finite dimension $d = 3$. The number of block states kept during the renormalization procedure was chosen step by step in order to avoid artificial symmetry breaking. This careful treatment insures that there are no spurious sources of asymmetry like partially taking into account a probability multiplet. Here we considered up to $m \simeq 300$ states in order to obtain stable results. Raw numerical data are shown in Fig. 2, where the finite-size dimerization parameter $D(L)$ is plotted as a function of the chain length L (see Eq. 5, and [28]). Finite-size scaling was used to extrapolate to the thermodynamic limit. After the extrapolation to the $L \rightarrow \infty$ limit, see Fig. 3, we fitted the dimer order parameter with a power law

$$D = \left(\frac{\theta - \theta_F}{\theta_0} \right)^\gamma \quad (6)$$

where $\gamma \sim 6.1502$ and $\theta_0 \sim 0.09177\pi$ (Fig. 3, solid line). We also tried to fit our data by an exponential law

$$D = D_0 e^{-a/\sqrt{\theta - \theta_F}} \quad (7)$$

as suggested in [18], with $a \sim 2.911$, $D_0 \sim 9.617$; this fit seems to work for narrower regions (Fig. 3, dashed line), however from our numerics we cannot exclude an exponential behavior of D in the critical region. The dimerized phase thus seems to survive up to the ferromagnetic phase boundary, independently from the chosen fitting form. This is also confirmed by the fact that the scaled gap between the ground state E_0 and the lowest excited state E_2 (which is found to have total spin $S_T = 2$) seems not to vanish in the interesting region $\theta > -0.75\pi$ (see inset of Fig. 3).

Moreover we analyzed the susceptibility of the chain to nematic ordering χ_{nem} . The numerical data, presented in Fig. 4, show a power law behavior $\chi_{\text{nem}}(L) \propto L^\alpha$ as a function of the system size. The exponent α (shown in the inset) approaches the value $\alpha = 3$ as $\theta \rightarrow \theta_F$. This can also be confirmed by means of a perturbative calculation around the exact solution available at θ_F ; indeed one obtains $|Q_{0,\gamma}|^2 \sim L^2$ and $(E_\gamma - E_0) \sim L^{-1}$ to be inserted in Eq. (4). The increase of the exponent for $\theta \rightarrow \theta_F$ indicates, as suggested in [21], that a tendency towards the nematic ordering is enhanced as the dimer order parameter goes to zero.

Conclusions - In this Letter we analyzed, by means of a DMRG analysis, the phase diagram of the one-dimensional spinor boson condensate on an optical lattice. We determined quantitatively the shape of the first two Mott lobes, and the even/odd properties of the lobes. We furthermore discussed the magnetic properties of the first lobe. Our results indicate that the Mott insulator is *always* in a dimerized phase.

This work was supported by IBM (2005 Faculty award), and by the European Community through grants RTNANO, SQUBIT2.

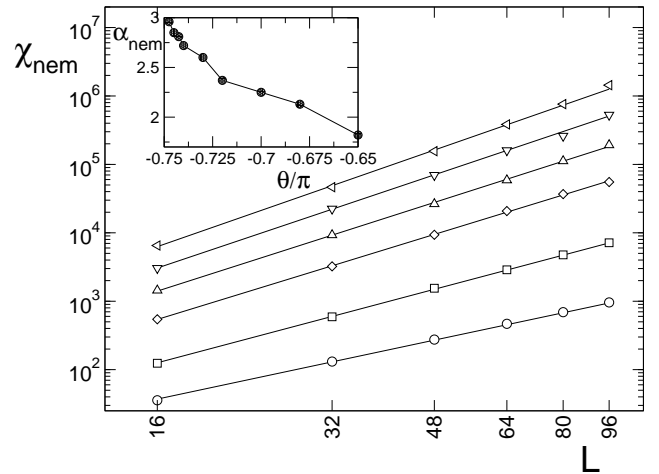


FIG. 4: Nematic susceptibility χ_{nem} as a function of the system size L . The various symbols refer to different values of θ : circles ($\theta = -0.65\pi$), squares (-0.7π), diamonds (-0.73π), triangles up (-0.74π), triangles down (-0.745π), triangles left (-0.7475π). Straight lines show a power law fit $\chi_{\text{nem}} = cL^\alpha$ of numerical data. Inset: exponent α as a function of θ .

* URL: qti.sns.it

- [1] B.P. Anderson and M.A. Kasevich, Science **282**, 1686 (1998); F.S. Cataliotti *et al.*, *ibid* **293**, 843 (2001); S. Burger *et al.*, Phys. Rev. Lett. **86**, 4447 (2001); O. Morsch *et al.*, *ibid* **87**, 140402 (2001).
- [2] D. Jaksch and P. Zoller; Ann. Phys. **315**, 52 (2005).
- [3] A. Minguzzi *et al.*, Phys. Rep. **395**, 223 (2004).
- [4] M. Greiner *et al.*, Nature **415**, 39 (2002).
- [5] D. Jaksch *et al.*, Phys. Rev. Lett. **81**, 3108 (1998).
- [6] M.P.A. Fisher *et al.*, Phys. Rev. B **40**, 546 (1989).
- [7] For a review of spinor condensates, see D.M. Stamper-Kurn and W. Ketterle, in *Coherent Atomic Matter Waves*, Proceedings of the Les Houches 1999 Summer School, Session LXXII, edited by R. Kaiser, C. Westbrook, and F. David (Springer, New York, 2001); cond-mat/0005001.
- [8] E. Demler and F. Zhou, Phys. Rev. Lett. **88**, 163001 (2002).
- [9] S.K. Yip, Phys. Rev. Lett. **90**, 250402 (2003).
- [10] A. Imambekov, M. Lukin, and E. Demler, Phys. Rev. A **68**, 063602 (2003).
- [11] F. Zhou and M. Snoek, Annals of Physics **308**, 692 (2003).
- [12] L.M. Duan, E. Demler, and M.D. Lukin, Phys. Rev. Lett. **91**, 090402 (2003).
- [13] A.A. Svidzinsky and S.T. Chui, Phys. Rev. A **68**, 043612 (2003).
- [14] A. Imambekov, M. Lukin, and E. Demler, Phys. Rev. Lett. **93**, 120405 (2004).
- [15] M. Snoek and F. Zhou, Phys. Rev. B **69**, 094410 (2004).
- [16] A.V. Chubukov, Phys. Rev. B **43**, 3337 (1991).
- [17] Y. Xian, J. Phys. Condens. Matter **5**, 7489 (1993).
- [18] G. Fàth and J. Sölyom, Phys. Rev. B **51**, 3620 (1995).
- [19] N. Kawashima, Prog. Theor. Phys. Suppl. **145**, 138

- (2002).
- [20] S. Tsuchiya, S. Kurihara, and T. Kimura, Phys. Rev. A **70** 043628 (2004).
 - [21] D. Porras, F. Verstraete, and J.I. Cirac, cond-mat/0504717.
 - [22] A. Läuchli, G. Schmid, and S. Trebst, cond-mat/0311082.
 - [23] J.J. García-Ripoll, M.A. Martin-Delgado, and J.I. Cirac, Phys. Rev. Lett. **93**, 250405 (2004).
 - [24] S.R. White, Phys. Rev. Lett. **69**, 2863 (1992); Phys. Rev. B **48**, 10345 (1993).
 - [25] T.D. Kühner and H. Monien, Phys. Rev. B **58**, R14741 (1998).
 - [26] T.D. Kühner, S.R. White, and H. Monien, Phys. Rev. B **61**, 12474 (2000).
 - [27] J. K. Freericks and H. Monien, Phys. Rev. B **53**, 2691 (1996).
 - [28] On any finite chain some inhomogeneity exists, thus leading to a finite D_L even if $D = 0$. Quantitatively, an order parameter D_L could be defined by evaluating Eq. (5) in the middle of the finite-size chain. The order parameter D has to be extrapolated in the limit $D \equiv \lim_{L \rightarrow \infty} D_L$.